Colloidal gelation, a means to study elasto-capillarity effects in foam

Alesya Mikhailovskaya,[a] Véronique Trappe[b] and Anniina Salonen *[a]

We explore the evolution of the mechanical properties of a coarsening foam containing colloidal particles that undergo a sol–gel transition in the continuous phase. This enables us to investigate the impact of elasto-capillarity on foam mechanics over a wide range of elasto-capillary numbers. Right after initiating aggregation the foam mechanics is predominantly determined by the elasticity of the bubbles, while the contributions of the continuous phase become dominant as the colloidal particles form a gel. Taking into account the confined configuration of the foam skeleton for the formation of a space spanning gel, we find that for elasto-capillary numbers exceeding unity the foam mechanics can be described as a simple linear combination of the contributions due to respectively the bubble elasticity and the elastic skeleton. Surprisingly, the contributions of the elastic skeleton to the overall foam mechanics are larger for smaller elasto-capillary numbers, scaling as the inverse of the capillary number.

Foams are densely packed assemblies of gas bubbles, in which the main part of the continuous phase is entrapped in a skeleton of vertices and Plateau borders. These two aspects form the base of diverse applications of foams, ranging from cosmetics to construction materials.[1,2] Indeed, we generally distinguish between liquid and solid foams, where liquid and solid refers to the state of the continuous phase.[1,3] The elasticity of a liquid foam is governed by bubble elasticity while the elasticity of solid foams is governed by the rigidity of the skeleton. In between these two extremes lies a wide range of foams, which cannot be easily classified as either liquid or solid.[4–8] The continuous phase is often weakly elastic, such that both the capillary stresses and the elasticity of the continuous phase play a role in determining the mechanical properties of the foam. This competition is captured in the elasto-capillary number $\mathrm{Ca_{el}}$ defined as $G_0 \Big/ \left(\frac{\gamma}{R}\right)$, with G_0 the shear modulus of the continuous phase, γ the surface tension and R the bubble size.[8–11]

From a mechanical point of view, the effect of adding bubbles or drops into an elastic material are fairly well understood.[11,12] By contrast, studies exploring the impact of weakly elastic continuous phases on foam mechanics are limited. Recently, Gorlier *et al.*[10] reported of such study, using dense emulsions as continuous phases to probe elasto-capillary numbers ranging from 0.4 to 30 by changing the emulsion elasticity and the bubble size. Their study indicated that the increase in elasticity of a foam due to the presence of an elastic continuous phase could be described by a unique function of the bubble volume fraction and the elasto-capillary number.

In this work we expand the range of elasto-capillary numbers investigated towards lower values. For this purpose, we exploit colloidal aggregation in the continuous phase of a SDS-stabilized foam. By probing the temporal evolution of the foam mechanics during the gelation process, we cover a range of $\mathrm{Ca_{el}} = 10^{-2}$–10 within a single experiment. Our experiments reveal that the foam elasticity can be described as a simple linear combination of the bubble elasticity and the elastic skeleton for $\mathrm{Ca_{el}} > 1$. By contrast, for $\mathrm{Ca_{el}} < 1$ the contribution of the weakly elastic skeleton on the overall foam mechanics is larger and scales as $\sim 1/\mathrm{Ca_{el}}$. Our results are distinct from those obtained for foams formed in dense emulsions,[10] which indicates that the extent of strengthening of a foam *via* an elastic continuous phase somewhat depends on the type of system used as continuous phase.

Experimental section

Sample

Our foam consists of bubbles that are fully stabilized by sodium dodecyl sulfate (SDS). The liquid fraction is set to $\varepsilon = 0.15$, which corresponds to the liquid fraction at which we can expect the impact of an elastic continuous phase on the overall elastic properties of the foam to be most pronounced.[10] As elastic continuous phase, we choose to use an aggregating colloidal

[a] *Université Paris-Saclay, CNRS, Laboratoire de Physique des Solides, 91405, Orsay, France. E-mail: anniina.salonen@universite-paris-saclay.fr*
[b] *Department of Physics, University of Fribourg, CH-1700 Fribourg, Switzerland*

system that exhibits elastic properties that slowly increase in time. The colloidal system is an aqueous suspension of silica particles (Ludox TMA) with particle diameter of 27 nm. At the start of any experiment, the conditions are set so that the final suspension contains 500 mM NaCl, 35 mM SDS and 17 wt% particles, the latter corresponding to a particle volume fraction of 8 v/v%.

Prior to final sample preparation, we prepare the following solutions:

– The pH of the initial stock suspension containing 34 wt% particles is adjusted to 6.8 by the dropwise addition of a NaOH solution with pH = 12. Once the pH is adjusted, the stock suspension is left to equilibrate for 2 days and used within 10 days.

– An aqueous SDS solution containing 555 mM SDS is prepared with Milli-Q water and used within a week to prevent hydrolysis of SDS.

– An aqueous solution of NaCl at a concentration of 4 M is prepared with Milli-Q water.

All materials used were purchased from Sigma-Aldrich and used without further purification.

To prepare an aggregating suspension for the study of the gelation process in a rheometer, we first mix the stock suspension, with Milli-Q water and SDS solution to obtain a preparation with 19.43 wt% particles and 40 mM SDS. The salt solution is then added to obtain the final conditions, briefly mixed using a vortex mixer, and immediately transferred to the rheometer. The moment the salt solution is added to the suspension is defined as $t = 0$.

To generate foams we use the two-syringe technique.[13] The setup consists of two disposable syringes coupled by a connector. The volume of each syringe is 60 mL and the diameter of their tips is 2 mm. For all preparations of foams with non aggregating continuous phases, we fill one syringe with the foaming solution and the other with air that has been bubbled through perfluorohexane C_6F_{14} (98+%, Alfa Aesar). The volumes of the liquid and gas phase are set so to obtain the desired liquid fraction of $V_{liquid}/(V_{gas} + V_{liquid}) = 0.15 \pm 0.01$. Pushing the syringes 15 times forward and backward ensures complete incorporation of the gas into the liquid. The moment of foam production is defined as $t = 0$. For the preparation of foams with an aggregating continuous phase, we ensure that the moment of foam production coincides with the moment at which the particle suspension becomes unstable by starting the foam production with one syringe filled with the particle suspension containing SDS and the other with the salt solution and the air containing traces of C_6F_{14}. All foams are immediately transferred to the rheometer or to test-tubes for further analysis.

All samples are prepared and investigated at a temperature of 26.0 ± 0.5 °C.

Rheometry

To follow the temporal evolution of the mechanical properties of foams with and without aggregating continuous phase and that of the aggregating particle suspension itself, we perform oscillatory strain experiments with commercial rheometers (Anton Paar MCR 300 and MCR 502). For the foam experiments, we use a home-made Couette cell with a gap size of 5.02 mm, which corresponds to at least 50 bubble diameters. The foams are loaded through a 5 mm hole at the bottom of the cup after lowering the cylinder to the measurement position, as done in ref. 14. For the experiments probing the aggregation of the particle system we use a standard Couette cell with a 1 mm gap, as well as a plate-plate geometry with various gap sizes. The storage $G'(\omega)$ and loss moduli $G''(\omega)$ are measured at a fixed frequency of $\omega = 10$ rad s^{-1} using strains within the linear range.

Microscopy

To follow the temporal evolution of the bubble radius, we proceed by diluting a portion of the foam after different coarsening times, using a SDS solution as diluting agent. The diluted sample is sandwiched between two coverslips that are spaced 150 μm from each other by using a spacer. Images of at least thousand bubbles are then taken by using a transmission microscope (Keyence VHX-2000) equipped with a digital camera, using either a 50× or 150× objective. The average bubble radius is retrieved by treating the images with ImageJ software.

Results and discussion

As denoted in the introduction, our goal is to explore the impact of an elastic continuous phase on the mechanical properties of foams. To scan a wide range of continuous phase elasticities we choose to study the temporal evolution of a foam containing colloidal particles that undergo a sol–gel transition.

Our foams have a liquid fraction of $\varepsilon \approx 0.15$ and they are fully stabilized by SDS. In the absence of a gelling continuous phase they are prone to coarsening and drainage. Colloidal gelation within the continuous phase suppresses drainage quickly after foam preparation, but not the coarsening process. As shown in the inset of Fig. 1(a), the mean bubble radius R increases in time independently of whether the continuous phase undergoes a sol–gel transition or not, the time t being here defined as the time elapsed since foam production. Due to traces of C_6F_{14} in the air used in the foam production the coarsening process is significantly slower than expected when using pure air. In the latter case we expect that $R \sim t^{1/2}$ [1] while we find $R \sim t^{1/5}$ for our foams. The reason for this is the low water solubility of C_6F_{14}. Because of this low solubility, the gas diffusing from small to large bubbles due to the difference in Laplace pressure is mainly composed of air. The coarsening process thus entails an increase of the osmotic pressure in the small bubbles and a decrease in the large bubbles, which opposes coarsening.[15]

A change in bubble size generally modifies the mechanical properties of a foam.[16] To be able to account for this we characterize the temporal evolution of the elasticity of the foam without gelling continuous phase by performing an oscillatory strain experiment at an angular frequency of 10 rad s^{-1} and a strain well within the linear range. As expected, the storage modulus G_f decreases in time, as shown in Fig. 1(a). To further

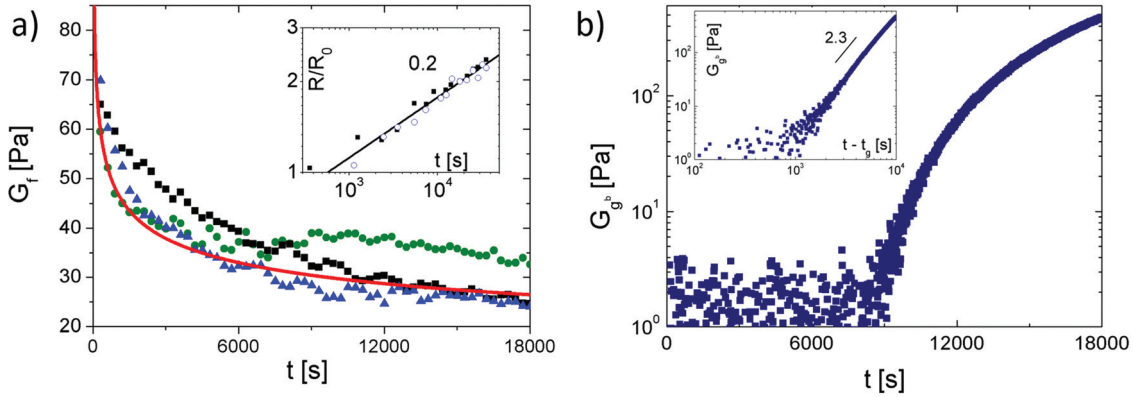

Fig. 1 Characteristics of foam and gel evolution. (a) Temporal evolution of the elastic modulus of SDS foams without gelling continuous phase: black squares denote the foam without any addition, green circles denote the foam containing 500 mM NaCl, blue triangles denote the foam containing 10 v/v% particles. The solid line corresponds to $G_f = \alpha(1-\varepsilon)(\varepsilon_{rcp}-\varepsilon)\gamma/R$. Inset: Temporal evolution of average bubble radius R normalized by the value R_0 = 25 μm obtained at t = 0 for a SDS foam without particles (black squares), and a gelling foam containing particles (blue circles). (b) Temporal evolution of elastic modulus of colloidal silica suspension after initiating aggregation by the addition of salt. Inset: Same data represented as a function of $t - t_g$.

test whether the sole presence of particles or salt would alter this development, we also explore the evolution of foams in the presence of either of both. As shown in Fig. 1(a), the elastic properties of these foams are within error bars the same as for the standard SDS foam, which indicates that the presence of particles or salt does not significantly modify the foam properties. As denoted by the red continuous line in Fig. 1(a), we find that the foam elasticity displays a dependence on bubble size, which is typical for foams for which elasticity arises purely from the bubble capillary pressure[16,17]

$$G_f = \alpha(1-\varepsilon)(\varepsilon_{rcp}-\varepsilon)\gamma/R \qquad (1)$$

ε is the foam liquid fraction, ε_{rcp} is the liquid fraction at random close packing, γ the surface tension of the SDS loaded water–air interface, γ = 37 mN m^{-1}, and α a dimensionless factor. Assuming for ε_{rcp} the value obtained for monodisperse foams, ε_{rcp} = 0.36, we find α = 0.2 to be significantly smaller than expected ($\alpha \approx 1.4$);[16] this is likely due to polydispersity, which generally entails that $\varepsilon_{rcp} < 0.36$.[18]

For the evolution of the elasticity of our foams with gelling continuous phases, called hereafter the gelling foam, we need to account for both the evolving capillary pressure and the evolution of the elastic properties of the continuous phase undergoing a sol–gel transition. To account for the latter, we investigate the gelation process of our colloidal silica suspension in bulk. The suspension is initially charge stabilized and we induce aggregation by increasing the ion concentration to 500 mM by the addition of a salt solution. The moment of adding the salt solution is defined as t = 0 and we follow the evolution of the elastic modulus, by performing oscillatory shear experiments at an angular frequency of 10 rad s^{-1} within the linear range at a strain of 0.002%. In the early stages of aggregation, the signal is too low to be resolved in our experiment. However, upon gelation the storage modulus rises sufficiently to be measurable and subsequently increases substantially, as shown in Fig. 1(b). Consistent with reaction-limited aggregation[19] we find that gelation is rather slow. The rate at which the elasticity increases beyond the gel-point is reasonably described by a critical-like power law, $G_{gb} \sim (t-t_g)^{2.3}$, as shown in the inset of Fig. 1(b). Though power law dependences of the elasticity on time are not unusual in colloidal gels, the exponents are generally found to be significantly lower, of the order of 1/3.[20–24] However, larger power law exponents are expected from percolation theory,[25] and we may conceive that the distinct behaviour observed for our gel is due to the reaction limited process governing the aggregation of our colloidal system, as opposed to the diffusion limited processes that govern the aggregation of most colloidal systems.

The temporal evolution of the elasticity of the gelling foam G_{gf} broadly reflects that expected from the evolution of both the standard foam and the gelling silica suspension. As shown in Fig. 2, the elastic modulus first decreases and then increases again, consistent with the idea that the coarsening induced decrease of the elastic modulus determines the evolution of G_{gf} at early times, while the increase in elasticity of the continuous phase determines the evolution of G_{gf} at a later stage. However, the comparison with the temporal evolution of the elasticity of the SDS foam denoted as red solid line in Fig. 2 reveals that aggregation and gelation in the continuous phase leads to an increase in the foam elasticity at remarkably early times. This is particularly intriguing considering that the gel-point as measured for the bulk gel is only reached at t_g = 8500 s, marked as bold circle in Fig. 2. As denoted in our study of the temporal evolution of the bubble size for the foams with and without a gelling continuous phase, the coarsening process of our foams is independent of the nature of the continuous phase (see inset of Fig. 1(a)). Moreover, we can infer from our study of the evolution of the elastic modulus of foams in the presence of respectively salt and particles that the sole presence of either of both does not significantly alter the surface tension (see main graph of Fig. 1(a)). The surface tension and the temporal evolution of the bubble size being the same for all foams investigated, it is thus reasonable to assume that the contribution of the bubble assembly to the elasticity of the gelling

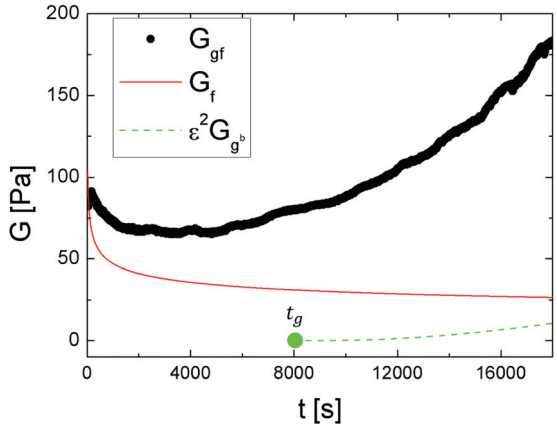

Fig. 2 Temporal evolution of the elastic modulus of SDS foams with gelling continuous phase denoted as black circles. For comparison the pure SDS foam is shown as red continuous line and the expected contribution of the gel phase as dashed green line. The gel point as measured in the 1 mm gap Couette geometry is marked as bold circle.

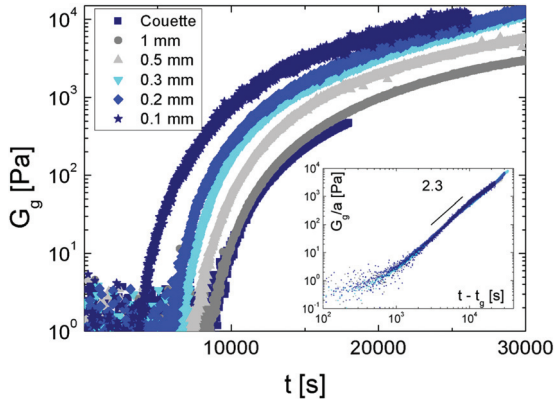

Fig. 3 Gap-size dependent gelation. Data obtained with a 1 mm Couette cell are denoted as black squares. All other data are obtained with a plate and plate geometry and gap sizes as indicated in the graph. Inset: Master curve obtained by normalizing G_g by a factor a and reporting the data as a function of $t - t_g$.

foams G_{gf} should correspond to that of the simple SDS foam. Modelling the bubbles by Kelvin cells we estimate that the fraction of liquid in the Plateau borders of our foam is $\sim$99%;[1] contributions of the films should thus be negligible. We can therefore consider the gelling foam as an open cell system that will exhibit an elasticity corresponding to the prediction of Gibson and Ashby[3] when $G_g \gg G_f$: $\varepsilon^2 G_{gb}$, where we denote with G_{gb} the elastic modulus of the bulk gel. The bulk gel contribution is shown as dashed line in Fig. 2. It remains small compared to G_f over the entire duration of our experiment such that the distinctly higher values of G_{gf} as compared to G_f appear somewhat surprising.

To account for this behaviour, we consider that the gelation process within the confined configuration of the foam may differ from that obtained in the 1 mm gap Couette geometry used to probe the evolution of the aggregating silica particles in bulk. To test this hypothesis we investigate the temporal evolution of the mechanical properties of our gelling suspensions using a plate and plate geometry varying the gap size from 1 mm to 0.1 mm. Remarkably, we find that the gel-time and the subsequent evolution of the elastic modulus indeed depends on gap-size, as shown in Fig. 3. Within error bars, the hallmarks of gelation observed by using a Couette geometry with a 1 mm gap are identical to those obtained using a 1 mm gap plate and plate geometry. This excludes gravity effects being at the origin of the observed gap dependence, as we would expect any effect of sedimentation to be markedly different in both geometries, the gravity direction being parallel to the shear plane in the Couette geometry, while it is perpendicular to the shear plane in the plate and plate geometry. An effect on gap size is somewhat unexpected, and to our knowledge has not been observed so far in colloidal gelation. It is suggestive of finite size scaling in percolation problems.[25] Let us note that the gap-size at which the 'finite size effect' becomes significant is of the order of 10^4 particle diameters, which is significantly larger than usually observed, finite size effects typically appearing when the system size is of 10–100 particle diameters. On a purely speculative base, we may envision that aggregation first leads to the formation of clusters, and that these clusters form the unit of a percolation problem. A full understanding of the origin of the gap size dependence is beyond the scope of this paper. For the assessment of the foam mechanics, it is sufficient to note that our experiments testing the effect of a one-dimensional confinement certainly indicate that the gel time is likely to be significantly smaller in the confining geometry of a foam than those measured in bulk. Based on the dependence of the gel time on the gap size shown in Fig. 4(a), we estimate the gel-times within the Plateau borders of our foams with diameters $\sim$8 μm to be of the order 360 s. It is important to note that while the gel time and the absolute magnitude of the elastic modulus depend on gap size, the functional development does not. As shown in the insets of Fig. 3, the time dependence of the gel elasticity obtained at different gap sizes can be scaled onto a single master-curve by reporting the data as a function of $(t - t_g)$ and by applying a normalization factor a to G_g to match the values obtained with a 1 mm gap. This scaling enables us to estimate the temporal development of the elastic modulus in the confining geometry of a Plateau border G_{gc}, by using t_g and a obtained by extrapolating the data shown in Fig. 4 to a gap size corresponding to the dimension of the Plateau borders.

Based on this extrapolation, we postulate that for gelation within the Plateau borders, $G_{gc}(t) = a \times B \times (t - t_g)^{2.3}$, with $a = 4.1$, $t_g = 360$ s and $B = 3 \times 10^{-7}$, B being obtained from the power-law fit of our reference experiment with $d_{gap} = 1$ mm (see inset Fig. 3). Using this time dependence for the elastic modulus of the gel, we find that $\varepsilon^2 G_{gc}(t)$ exhibits a time dependence that follows the long time limit of $G_{gf}(t)$, as shown in Fig. 5. Assuming that the elasticity of the gelling foam can be modelled as a parallel connection of two elastic elements with elastic constants corresponding respectively to the bubble capillary pressure and the open cell elasticity, we can write

$$G_{gf}(t) = G_f(t) + \varepsilon^2 G_{gc}(t) \qquad (2)$$

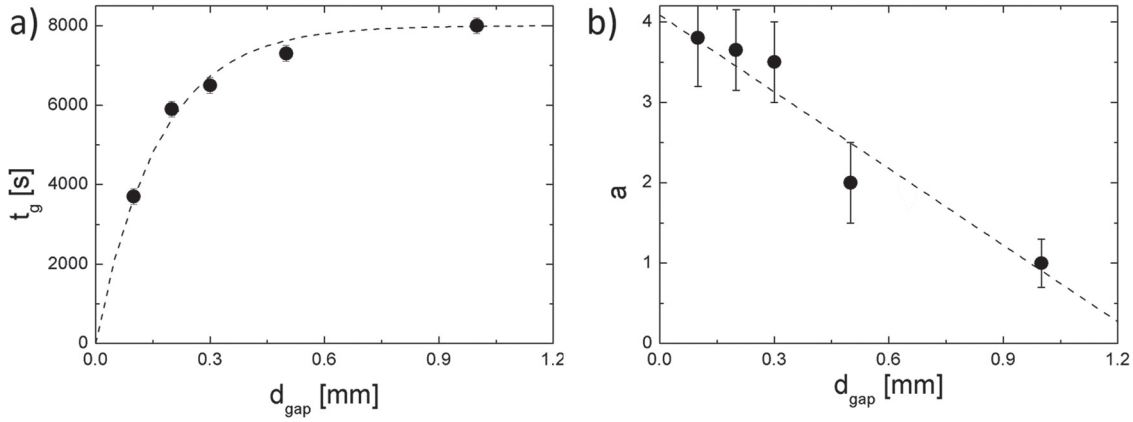

Fig. 4 (a) Gap size dependence of the gel time t_g. The dashed line corresponds to an empirical description of the data: $t_g = t_{g,\infty}(1 - \exp\{d_{gap}/0.17\})$ with $t_{g,\infty} = 8000$ s. (b) Gap size dependence of the factor a used to normalize the elastic modulus in the inset of Fig. 3. The dashed line corresponds to a linear fit, $a = 4.1 - 3.2d_{gap}$.

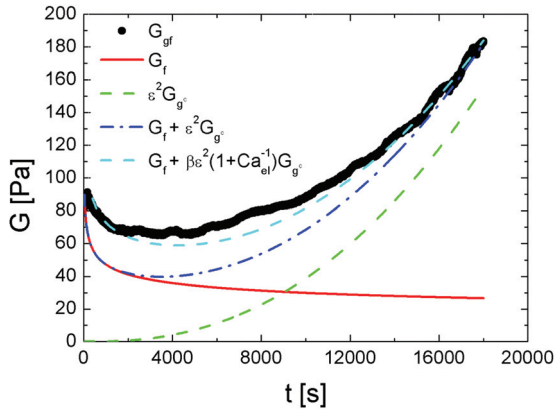

Fig. 5 Same data as in Fig. 2. Red continuous line denotes the evolution of G_f, the green dashed line denotes the expected contributions of the gel phase when accounting for finite size effects, and the dark blue dashed dotted line corresponds to the addition of both contributions according to eqn (2). The light blue dashed line is the description of the data assuming that the weight of the elastic continuous phase depends inversely on the elasto-capillary number (see text).

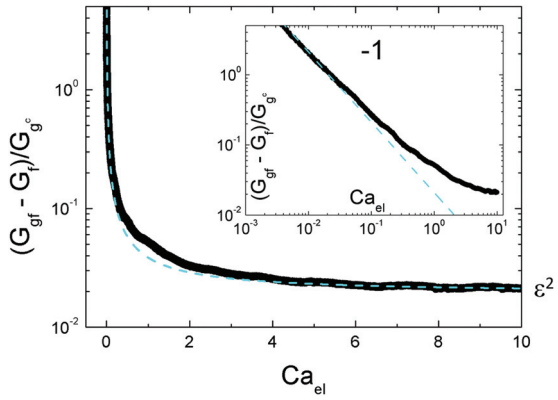

Fig. 6 Weight of the gel contribution x in $G_{gf} = G_f + xG_{g^c}$ shown as a function of the elasto-capillary number. The behaviour expected from the Gibson and Ashby prediction for open cell solid foams, $x = \varepsilon^2$, is reached at high Ca_{el}. At lower Ca_{el}, $x \propto 1/Ca_{el}$, as shown in the inset. The dashed light blue line describing the data over the entire range of elasto-capillary numbers investigated corresponds to $(G_{gf} - G_f)/G_{g^c} = \beta(1 + Ca_{el}^{-1})\varepsilon^2$.

This simple additive model, shown as dark blue dashed dotted line in Fig. 5, reasonably describes the data at long times on an absolute scale, but it fails accounting for the large discrepancy between G_{gf} and G_f at shorter times when $G_f > G_{g^c}$. At this condition, the elasticity of the continuous phase or more precisely the Plateau borders and nodes seems to lead to an increase of the foam elasticity that is significantly larger than one would expect assuming a simple additive effect. This broadly agrees with the behaviour observed for foams with elastic continuous phases made of dense emulsions. Indeed Gorlier *et al.* proposed to add a coupling term to eqn (2) to describe the elasticity of their foams.[10] The coupling term linearly depending on the elasticity of the continuous phase, this amounts to assuming that the weight of G_{g^c} in eqn (2) is not fixed but varies in time, $G_{gf}(t) = G_f(t) + x(t)G_{g^c}(t)$. More precisely we can assume that x depends on the elastic capillary number, $Ca_{el} = G_{g^c}/(R/\gamma)$, a ratio describing the relative resistances to deformation of respectively the gel and the bubble on a local scale. As shown in Fig. 6, $x = (G_{gf}(t) - G_f(t))/G_{g^c}(t)$ exhibits a distinct dependence on Ca_{el}. For $Ca_{el} > 1$, $(G_{gf}(t) - G_f(t))/G_{g^c}(t)$ reaches the limit expected from the open cell model ε^2. For $Ca_{el} < 1$, $(G_{gf}(t) - G_f(t))/G_{g^c}(t)$ is approximately inversely proportional to Ca_{el}, as denoted in the double logarithmic plot shown in the inset of Fig. 6. In fact, we find that the elasticity of the gelling foam is reasonably described assuming $x = 0.92(1 + Ca_{el}^{-1})\varepsilon^2$ (light blue dashed line in Fig. 5 and 6) This description is purely empirical, and differs from that reported by Gorlier *et al.* who found that the behaviour of their foam with $\varepsilon = 0.15$ was best described with $x = (1 + 10.5Ca_{el}^{-2/3})\varepsilon^2$ for $Ca_{el} \geq 0.5$.[10]

To further compare the mechanical properties of foams with elastic continuous phases composed of respectively colloidal gels and dense emulsions, we show in Fig. 7 the factorial increase of the foam elasticity due to the presence of an elastic continuous phase $G(Ca_{el})/G_f$ as a function of Ca_{el}. Note that $G(Ca_{el}) = G_{gf}$ in the case of the gelling foam. Clearly, the

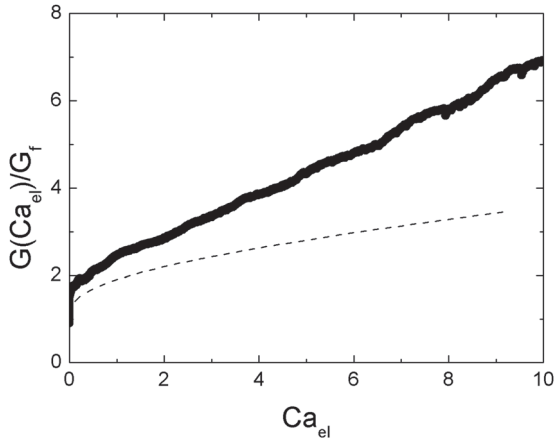

Fig. 7 Fractional increase of foam elasticity due to the presence of an elastic continuous phase, $G(Ca_{el})/G_f$, as a function of the elasto-capillary number, for foams with a liquid fraction of $\varepsilon = 0.15$. The black circles denote the data obtained for the foam with the gel continuous phase (this work, $G(Ca_{el}) = G_{gf}$), the black dashed line denote the behaviour found by Gorlier *et al.*[10] for foams with elastic continuous phases made of dense emulsions.

efficiency of a colloidal gel in increasing the foam elasticity is larger than that of a dense emulsion. One may conceive that this difference arises from the different pathways of providing elasticity to the foam interstices. The gel is formed within the foam interstices, while the glassy emulsion is forced into the interstices during foam production. It is thus likely that the gel couples more efficiently to the local bubble configuration than the glassy emulsions droplets.

These findings certainly indicate that foam elasticity is not a unique function of the elasto-capillary number, but also depends on the system used as a continuous phase. Let us note that the elasto-capillary number is nonetheless an interesting parameter. In the case of the gelling foam it denotes a transition at $Ca_{el} \approx 1$ between the parameter space in which the foam elasticity rises very quickly with increasing Ca_{el} before exhibiting a linear increase consistent with the simple additive model denoted in eqn (2). More investigations will be needed to fully elucidate this trend. However, if confirmed, this would indicate that the foam elasticity can be efficiently increased by using even a very weak elastic continuous phase.

Conclusion

In conclusion, our work on the mechanical properties of gelling foams discloses two distinct findings.

The first relates to colloidal gelation at conditions at which we usually consider aggregation to be reaction limited,[26,27] namely in the case of colloidal aggregation in suspensions of charged colloids exhibiting a DLVO-potential with a finite repulsive barrier.[28,29] Our experiments reveal considerable confinement effects; they denote a decrease of the gel-time with increasing confinement, consistent with finite size effects in percolation theory.[25] Further evidence that the gelation process in our systems is broadly consistent with that predicted by percolation theory is found in the evolution of the elastic modulus beyond the gel-point. In this post-gel regime, particles and finite clusters become part of the percolated structure as the bonding probability increases. In our experiments the bonding probability increases in time, and we find that the elastic modulus increases as function of $(t - t_c)^s$ with, $s \approx 2.3$, an exponent that is within the range of exponents predicted by percolation theory.[25]

With respect to foams with elastic continuous phases, our experiment probing the mechanical properties of a foam with a continuous phase containing colloidal particles that undergo a sol–gel transition allowed us to probe the effects of an elastic interstitial material over a wide range of elasticities. The main finding is here that the development of the mechanical properties of the foam with increasing interstitial elasticity exhibits distinct features. For elasto-capillary numbers exceeding unity the foam mechanics is well described by a simple additive model accounting for the contributions of the bubble assembly and that of an open cell elastic structure. However, for elasto-capillary numbers below one the effect of an elastic skeleton is significantly larger than predicted by such simple additive model. Exploring the exact origin of this enhanced impact of weakly elastic continuous phases on foam elasticity remains a topic of future research.

Conflicts of interest

There are no conflicts to declare.

Acknowledgements

We thank Emanuela Del Gado, Dominique Langevin, François Lavergne, Cyprien Gay, Olivier Pitois and Robert Style for fruitful discussions. Funding from European Space Agency (Hydrodynamics of wet foams) and the Swiss Science Foundation (grant number 200021_172514) are gratefully acknowledged.

References

1 I. Cantat, S. Cohen-Addad, F. Elias, F. Graner, R. Höhler; O. Pitois, F. Rouyer and A. Saint Jalmes, *Les Mousses: Structure et Dynamique*, Belin, 2011.
2 C. Hill and J. Eastoe, Foams: From Nature to Industry, *Adv. Colloid Interface Sci.*, 2017, **247**, 496–513, DOI: 10.1016/j.cis.2017.05.013.
3 L. J. Gibson and M. F. Ashby, *Cellular Solids: Structure and Properties*, Cambridge, 1997.
4 R. M. Guillermic, A. Salonen, J. Emile and A. Saint-Jalmes, Surfactant Foams Doped with Laponite: Unusual Behaviors Induced by Aging and Confinement, *Soft Matter*, 2009, **5**(24), 4975–4982, DOI: 10.1039/b914923f.
5 J. Goyon, F. Bertrand, O. Pitois and G. Ovarlez, Shear Induced Drainage in Foamy Yield-Stress Fluids, *Phys. Rev. Lett.*, 2010, **104**(12), 128301.
6 A. Salonen, R. Lhermerout, E. Rio, D. Langevin and A. Saint-Jalmes, Dual Gas and Oil Dispersions in Water: Production

and Stability of Foamulsion, *Soft Matter*, 2012, **8**(3), 699–706, DOI: 10.1039/c1sm06537h.

7 I. Lesov, S. Tcholakova and N. Denkov, Drying of Particle-Loaded Foams for Production of Porous Materials: Mechanism and Theoretical Modeling, *RSC Adv.*, 2014, **4**(2), 811–823, DOI: 10.1039/c3ra44500c.

8 L. Ducloué, O. Pitois, J. Goyon, X. Chateau and G. Ovarlez, Coupling of Elasticity to Capillarity in Soft Aerated Materials, *Soft Matter*, 2014, **10**(28), 5093, DOI: 10.1039/c4sm00200h.

9 L. Ducloué, O. Pitois, J. Goyon, X. Chateau and G. Ovarlez, Rheological Behaviour of Suspensions of Bubbles in Yield Stress Fluids, *J. Nonnewton. Fluid Mech.*, 2015, **215**, 31–39, DOI: 10.1016/j.jnnfm.2014.10.003.

10 F. Gorlier, Y. Khidas and O. Pitois, Coupled Elasticity in Soft Solid Foams, *J. Colloid Interface Sci.*, 2017, **501**, 103–111, DOI: 10.1016/j.jcis.2017.04.033.

11 M. Kogan, L. Ducloue, J. Goyon, X. Chateau, O. Pitois and G. Ovarlez, Mixtures of Foam and Paste: Suspensions of Bubbles in Yield Stress Fluids, *Rheol. Acta*, 2013, **52**(3), 237–253, DOI: 10.1007/s00397-013-0677-7.

12 R. W. Style, R. Boltyanskiy, B. Allen, K. E. Jensen, H. P. Foote, J. S. Wettlaufer and E. R. Dufresne, Stiffening Solids with Liquid Inclusions, *Nat. Phys.*, 2015, **11**(1), 82–87, DOI: 10.1038/nphys3181.

13 T. Gaillard, M. Roché, C. Honorez, M. Jumeau, A. Balan, C. Jedrzejczyk and W. Drenckhan, Controlled Foam Generation Using Cyclic Diphasic Flows through a Constriction, *Int. J. Multiphase Flow*, 2017, **96**, 173–187, DOI: 10.1016/j.ijmultiphaseflow.2017.02.009.

14 A. D. Gopal and D. J. Durian, Relaxing in Foam, *Phys. Rev. Lett.*, 2003, **91**(18), 188303, DOI: 10.1103/PhysRevLett.91.188303.

15 D. Weaire and V. Pageron, Frustrated Froth: Evolution of Foam Inhibited by an Insoluble Gaseous Component, *Philos. Mag. Lett.*, 1990, **62**(6), 417–421, DOI: 10.1080/09500839008215544.

16 S. Cohen-Addad, R. Höhler and O. Pitois, Flow in Foams and Flowing Foams, *Annu. Rev. Fluid Mech.*, 2013, **45**(1), 241–267, DOI: 10.1146/annurev-fluid-011212-140634.

17 T. G. Mason, J. Bibette and D. A. Weitz, Elasticity of Compressed Emulsions, *Phys. Rev. Lett.*, 1995, **75**(10), 2051–2054, DOI: 10.1103/PhysRevLett.75.2051.

18 V. Baranau and U. Tallarek, Random-Close Packing Limits for Monodisperse and Polydisperse Hard Spheres, *Soft Matter*, 2014, **10**(21), 3826–3841, DOI: 10.1039/c3sm52959b.

19 M. Y. Lin, H. M. Lindsay, D. A. Weitz, R. C. Ball, R. Klein and P. Meakin, Universal Reaction-Limited Colloid Aggregation, *Phys. Rev. A: At., Mol., Opt. Phys.*, 1990, **41**(4), 2005–2020, DOI: 10.1103/PhysRevA.41.2005.

20 S. Manley, B. Davidovitch, N. R. Davies, L. Cipelletti, A. E. Bailey, R. J. Christianson, U. Gasser, V. Prasad, P. N. Segre and M. P. Doherty, *et al.*, Time-Dependent Strength of Colloidal Gels, *Phys. Rev. Lett.*, 2005, **95**(4), 048302, DOI: 10.1103/PhysRevLett.95.048302.

21 N. Koumakis and G. Petekidis, Two Step Yielding in Attractive Colloids: Transition from Gels to Attractive Glasses, *Soft Matter*, 2011, **7**, 2456–2470, DOI: 10.1039/c0sm00957a.

22 H. Guo, S. Ramakrishnan, J. L. Harden and R. L. Leheny, Gel Formation and Aging in Weakly Attractive Nanocolloid Suspensions at Intermediate Concentrations, *J. Chem. Phys.*, 2011, **135**(15), 154903, DOI: 10.1063/1.3653380.

23 D. C. E. Calzolari, I. Bischofberger, F. Nazzani and V. Trappe, Interplay of Coarsening, Aging, and Stress Hardening Impacting the Creep Behavior of a Colloidal Gel, *J. Rheol.*, 2017, **61**(4), 817–831, DOI: 10.1122/1.4986465.

24 S. Aime, L. Cipelletti and L. Ramos, Power Law Viscoelasticity of a Fractal Colloidal Gel, *J. Rheol.*, 2018, **62**(6), 1429–1441, DOI: 10.1122/1.5025622.

25 D. Stauffer, A. Coniglio and M. Adam, Gelation And Critical Phenomena, *Polymer networks*, Springer, Berlin, Heidelberg, 1982, pp. 103–158, DOI: 10.1007/3-540-11471-8_4.

26 P. Meakin and F. Family, Structure and Kinetics of Reaction-Limited Aggregation, *Phys. Rev. A: At., Mol., Opt. Phys.*, 1988, **38**(4), 2110–2123, DOI: 10.1103/PhysRevA.38.2110.

27 R. C. Ball, D. A. Weitz, T. A. Witten and F. Leyvraz, Universal Kinetics in Reaction-Limited Aggregation, *Phys. Rev. Lett.*, 1987, **58**(3), 274–277, DOI: 10.1103/PhysRevLett.58.274.

28 W. B. Russel, D. A. Saville and W. R. Schowalter, *Colloidal Dispersions*, Cambridge University Press, 1989.

29 J. N. Israelachvili, *Intermolecular and Surface Forces*, 3rd edn, 2011, DOI: 10.1016/C2011-0-05119-0.